

Supporting Information

Kinetic and equilibrium binding characterization of aptamers to small molecules using a label-free, sensitive, and scalable platform

Andrew L. Chang[†], Maureen McKeague[‡], Joe C. Liang[‡], Christina D. Smolke[‡]

[†]Department of Chemistry, Stanford University, Stanford, CA 94305

[‡]Department of Bioengineering, Stanford University, 473 Via Ortega, MC 4201, Stanford, CA 94305

Additional Materials and Methods

Figure S1. Representative SPR sensorgrams for *in vitro* selected aptamers

Figure S2. Representative SPR sensorgrams for natural RNA aptamers

Figure S3. Theophylline aptamer capture to the sensor chip and resulting theophylline binding response with varying aptamer concentrations

Figure S4. Correlation analysis of dissociation constants and reported selection immobilization concentrations for *in vitro* selected aptamers

Table S1. Summary of aptamer template sequences used in this work

Supporting Information References

Additional Materials and Methods

Nucleic acid aptamer preparation

DNA aptamer template sequences (Table S1, Supporting Information) were purchased from Integrated DNA Technologies (Coralville, IA). Oligonucleotides for DNA aptamers contain a 3' 24-mer poly(A) sequence and were directly used in the binding assay. Oligonucleotides for RNA aptamers contain a 5' T7 promoter and a 3' 24-mer poly(A) sequence. RNA aptamers were prepared by PCR amplification of templates using forward and reverse primers Biacore-fwd (5'-TTCTAATACGACTCACTATAGGG) and Biacore-rev (5'-TTTTTTTTTTTTTTTTTTTTTTTTTTTGGGG), respectively, followed by transcription of the PCR product using the MEGAscript T7 Kit (Life Technologies, Carlsbad, CA) and purification of the transcription product using the RNA Clean & Concentrator kit (Zymo Research, Irvine, CA), according to the manufacturers' instructions. In all experiments the HBS-N running buffer (10 mM HEPES, 150 mM NaCl, pH 7.4) (GE Healthcare, Uppsala, Sweden) was supplemented with the appropriate MgCl₂ concentration (Life Technologies). Nucleic acid aptamers were resuspended in running buffer, denatured at 65 °C for 5 min, and cooled to room temperature directly before use.

Sensor chip surface generation

Experiments were performed on a Biacore X100 instrument (GE Healthcare) at 25 °C. A CM5 sensor chip (GE Healthcare) was equilibrated with HBS-N buffer. The DNA linker strand (5'-AmMC6-TTTTTTTTTTTTTTTTTTTTTTTT) (Integrated DNA Technologies), with an amino modified 6-carbon linker on the 5' end, was immobilized to the chip surface. The carboxymethylated dextran surface of the CM5 chip was activated for 7 min at a flow rate of 10 µL/min using a 1:1 volume ratio of 0.4 M 1-ethyl-3-(3-dimethylaminopropyl) carbodiimide (GE Healthcare) and 0.1 M N-hydroxysuccinimide (GE Healthcare). A molar ratio of 1:30 of DNA strand to hexadecyltrimethylammonium bromide (Sigma-Aldrich, St. Louis, MO) was diluted in 10 mM HEPES buffer (Sigma-Aldrich) to a final concentration of 20 µM and 0.6 mM, respectively, and injected over the activated surface for 10 min at a flow rate of 5 µL/min. Excess activated groups were blocked by an injection of 1 M ethanolamine (GE Healthcare), pH 8.5, for 7 min at a flow rate of 10 µL/min. The immobilization reaction was performed sequentially on both flow cells (FC1, FC2) and yielded approximately 4,000 RU of the DNA strand.

Aptamer binding assay

The Biacore X100 instrument was primed three times with running buffer prior to all binding assays. For each assay, three startup cycles were performed to stabilize the sensorgram baseline. For each startup cycle, the aptamer (~40–70 ng/µL, ~3 µM) was captured onto the sample flow cell (FC2) for 40 s at a flow rate of 5 µL/min. The resulting capture levels between ~2,000–5,000 RU ensured maximum binding response by the small molecule (Figure S3, Supporting Information). 25 mM NaOH (GE Healthcare) was injected for 30 s at a flow rate of 30 µL/min over both flow cells to regenerate the sensor surface. A dilution series of the target was prepared in running buffer and filtered through a 0.2 µm membrane (Pall Corporation, Port

Washington, NY), using a minimum of nine concentrations spanning the 0.2–0.8 binding saturation range for steady-state affinity analysis. For each concentration sample, the aptamer was captured onto the sample flow cell (FC2) for 40 s at a flow rate of 5 $\mu\text{L}/\text{min}$, the target solution was injected over both flow cells at a flow rate of 30 $\mu\text{L}/\text{min}$ to monitor target association, and running buffer was injected over both flow cells at a flow rate of 30 $\mu\text{L}/\text{min}$ to monitor target dissociation. Association and dissociation phase lengths used for each target were chosen based on time needed to reach equilibrium (Figure 1B; Figures S1 and S2, Supporting Information). Aptamer and target were removed from the sensor surface by injecting 25 mM NaOH for 30 s at a flow rate of 30 $\mu\text{L}/\text{min}$ over both flow cells. Bis-(3'-5')-cyclic dimeric guanosine monophosphate (c-di-GMP) was purchased from Axxora, LLC (Farmingdale, NY); tyrosine was purchased from EMD Millipore (Billerica, MA); arginine, adenosine triphosphate (ATP), citrulline, flavin mononucleotide, glycine, malachite green, theophylline, and thiamine pyrophosphate (TPP) were purchased from Sigma-Aldrich.

Data processing and analysis were performed using Biacore X100 Evaluation Software version 2.0 (GE Healthcare). A double-referencing method was performed to process all datasets¹. Data from the sample flow cell (FC2) were referenced first by subtracting data from the reference flow cell (FC1) to correct for bulk refractive index changes, nonspecific binding, injection noise, matrix effects, and baseline drift. Reference-subtracted data (FC2 – FC1) were double-referenced with a blank injection of running buffer to account for any systematic drift over the course of the injection. Double-referenced data were fit to a 1:1 binding model for kinetic analysis or steady-state affinity model for thermodynamic analysis. Reported values are the mean and standard deviation of at least three independent experiments.

Figure S1. Representative SPR sensorgrams for *in vitro* selected aptamers.

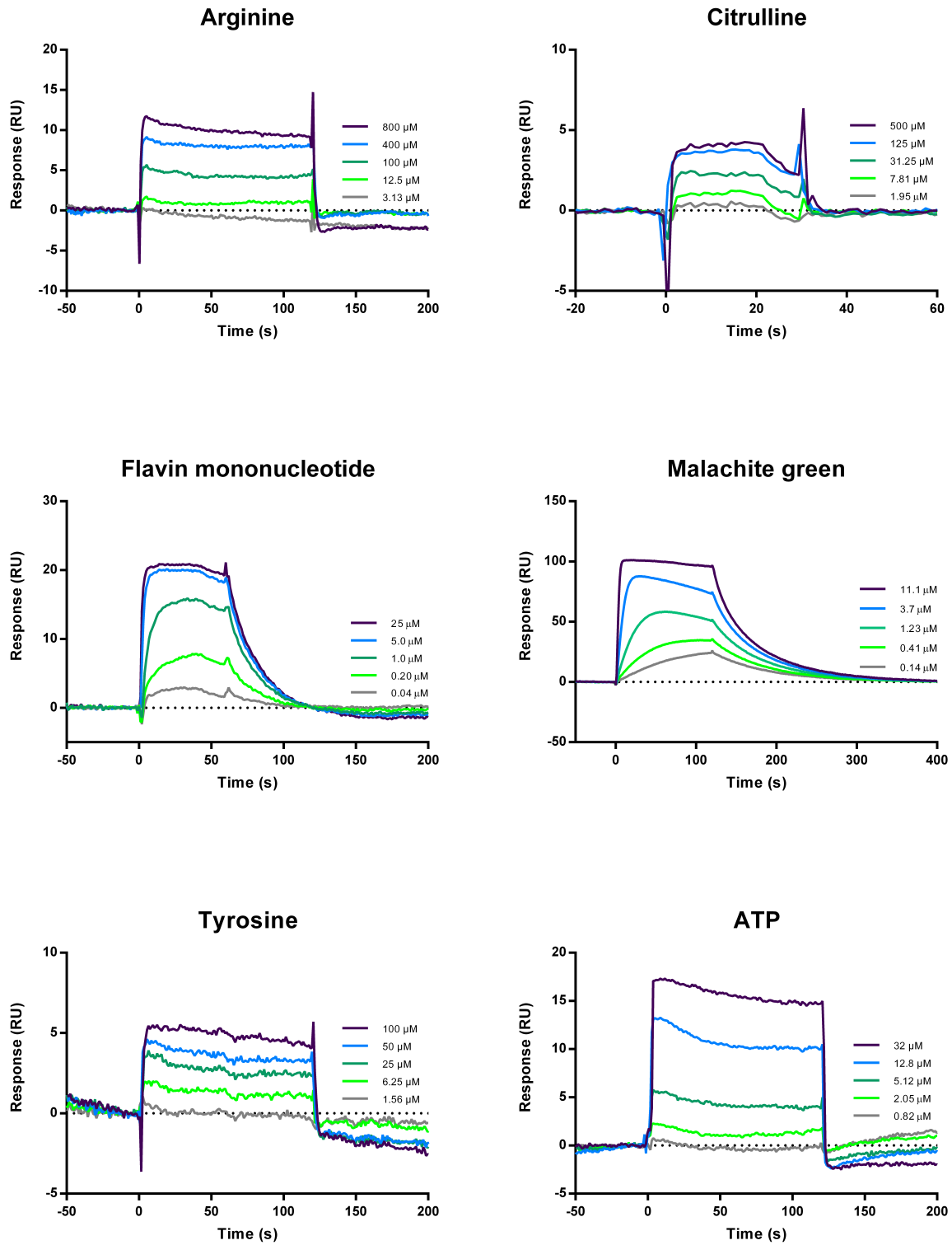


Figure S2. Representative SPR sensorgrams for natural RNA aptamers. c-di-GMP (class I) was characterized using single cycle kinetics by sequentially injecting increasing c-di-GMP concentrations with an extended dissociation to measure the slow dissociation rate (first panel).

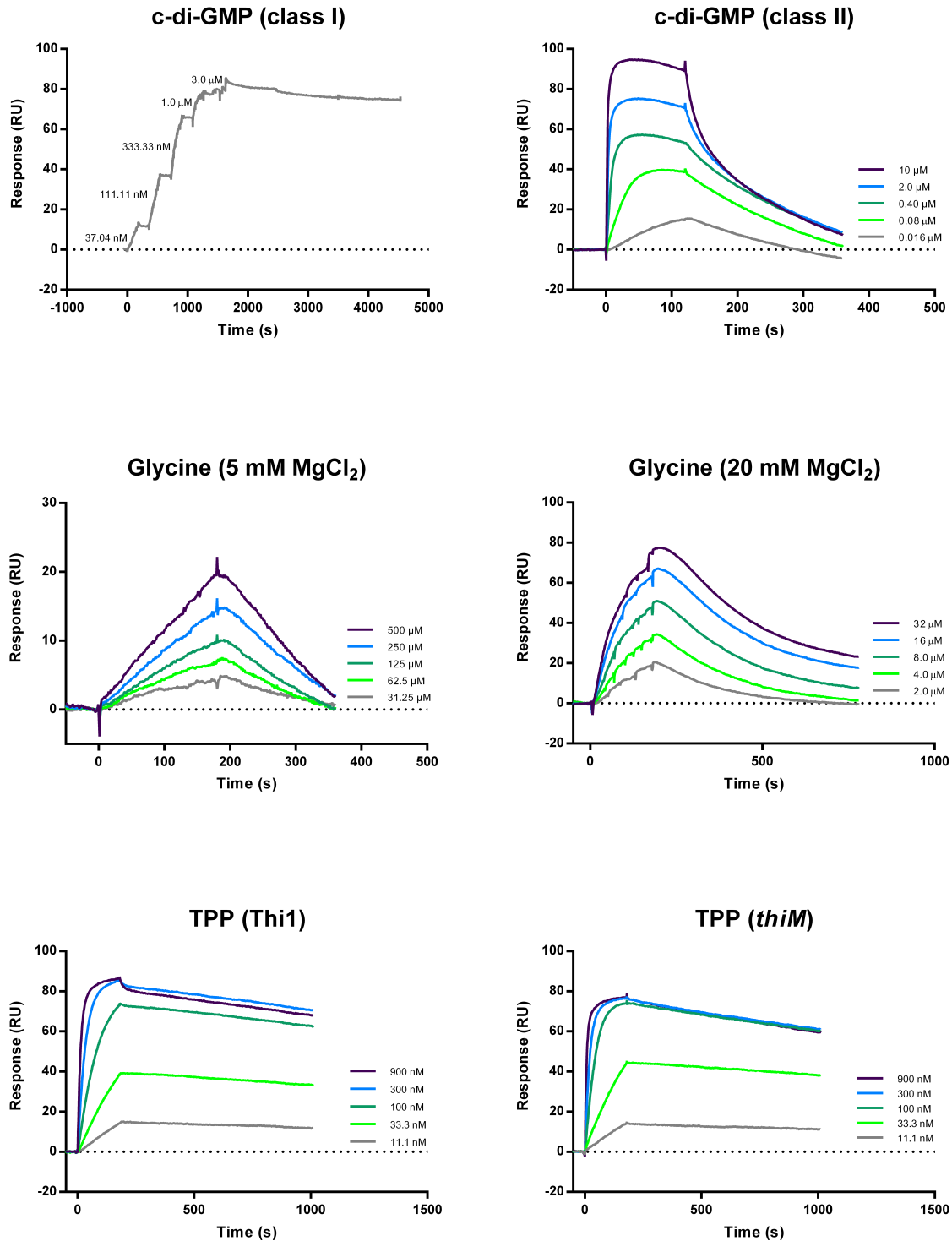


Figure S3. Theophylline aptamer capture to the sensor chip and resulting theophylline binding response with varying aptamer concentrations. A constant theophylline concentration of 0.3 μM , near the reported K_D , was used to determine the ideal aptamer concentration and corresponding capture level required to detect maximum theophylline binding. Aptamer capture levels greater than 2000 RU, corresponding to a minimum of 1.5 μM theophylline aptamer, resulted in maximum theophylline binding response (~ 20 RU) for the theophylline concentration used. Below this aptamer capture level, theophylline binding response decreases and approaches the limit of detection (LOD). As each aptamer and small molecule pair varies in size and measurable response, a slight excess of aptamer (~ 3 μM) was used in subsequent experiments to achieve maximum small molecule binding. The limit of detection of this method was calculated² as $\text{LOD} = \text{mean}_{\text{blank}} + 3.29(\text{SD}_{\text{blank}})$.

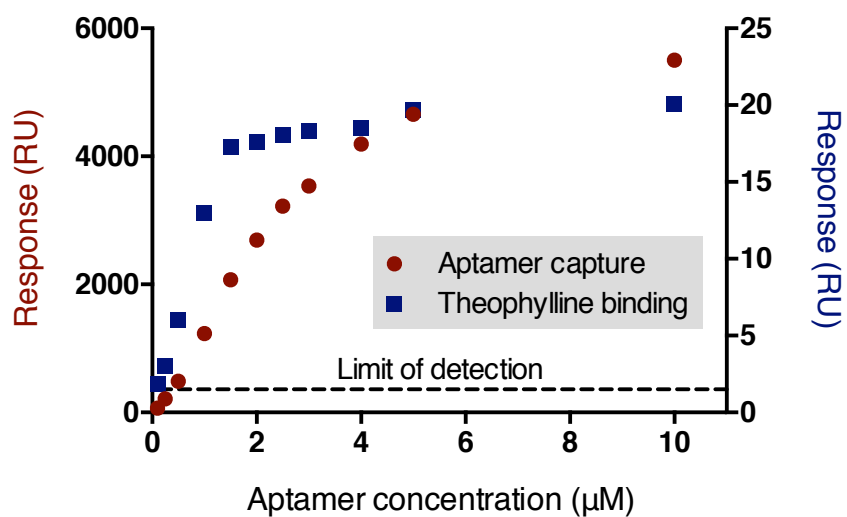
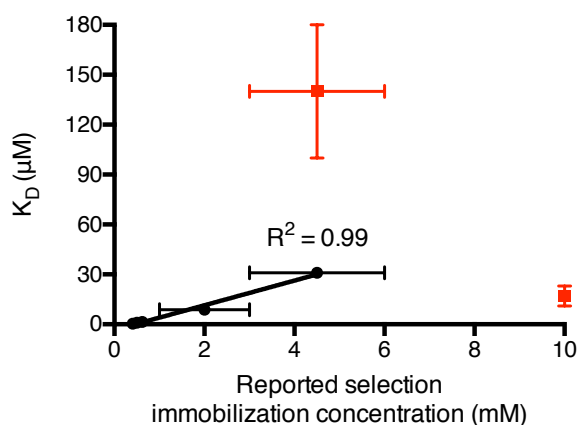


Figure S4. Correlation analysis of dissociation constants and reported selection immobilization concentrations for *in vitro* selected aptamers. Arginine and tyrosine aptamers are excluded from this analysis and are indicated in red. Reported selection immobilization concentration values plotted and x-axis error bars represent the midpoints and ranges of immobilization concentrations used in the *in vitro* selection experiments. The four aptamers that exhibit low- to mid-micromolar affinities and reach equilibrium quickly were selected by affinity chromatography on columns derivatized with millimolar concentrations of conjugated target, potentially a result of selection bias for fast binders that sample multiple targets. In contrast, *in vitro* selected aptamers with affinities in the mid-nanomolar to low-micromolar range were selected on columns with submillimolar concentrations of immobilized target.



Immobilized Target	Reported Selection Immobilization Concentration (mM) [†]	K_D [‡]
1-Carboxypropyl Theophylline ³	0.41	390 ± 20 nM
Flavin Mononucleotide ⁴	0.5	910 ± 200 nM
Malachite Green Isothiocyanate ⁵	0.62	1.5 ± 0.2 μM
ATP ⁶	1–3	8.8 ± 3 μM
Citrulline ⁷	3–6	31 ± 1 μM
Arginine ⁷	3–6	140 ± 40 μM
Tyrosine ⁸	10	17 ± 6 μM

[†] Reported concentrations represent either concentrations used in immobilization reactions or the final concentrations of conjugated target.

[‡] For arginine, citrulline, tyrosine, and ATP aptamers, $K_{D, \text{equilibrium}}$ values from Table 1 are plotted. For flavin mononucleotide, malachite green, and theophylline aptamers, plotted K_D values and y-axis error bars are the mean of $K_{D, \text{kinetic}}$ and $K_{D, \text{equilibrium}}$ values from Table 1 and propagated errors of $K_{D, \text{kinetic}}$ and $K_{D, \text{equilibrium}}$ measurements, respectively.

Table S1. Summary of aptamer template sequences used in this work. The ATP sequence was used without modification. All other sequences were transcribed into RNA before use. Forward primer constant regions are in bold and contain a T7 promoter sequence. Reverse primer constant regions are underlined and contain a poly(A) sequence and a short spacer of four cytosines to base pair with 5' guanines included to facilitate RNA transcription.

Target	Sequence
Arginine	TTCTAATACGACTCACTATAGGG ACGAGAAGGAGCGCTGGTTATA CTAGCAGGTAGGTCACTCGT <u>CCCCAAAAAAAAAAAAAAAAAAAA</u> <u>AAA</u>
Citrulline	TTCTAATACGACTCACTATAGGG ACGAGAAGGAGTGCTGGTTATA CTAGCGGTTAGGTCACTCGT <u>CCCCAAAAAAAAAAAAAAAAAAAA</u> <u>AAA</u>
Flavin Mononucleotide	TTCTAATACGACTCACTATAGGG CGTGTAGGATATCGTGTTGAG AAGGACACGCC <u>CCCCAAAAAAAAAAAAAAAAAAAA</u>
Malachite Green	TTCTAATACGACTCACTATAGGG ATCCCGACTGGCGAGAGCCAGG TAACGAATGGAT <u>CCCCAAAAAAAAAAAAAAAAAAAA</u>
Theophylline	TTCTAATACGACTCACTATAGGG AAGTGATACCAGCATCGTCTTG ATGCCCTTGGCAGCACTT <u>CCCCAAAAAAAAAAAAAAAAAAAA</u> <u>A</u>
Tyrosine	TTCTAATACGACTCACTATAGGG GGCAGTCAACTCGTAAGATGGC CTTACAGCGGTCAATACGGGGGTCATCAGATAGGGAGGCC <u>CCCC</u> <u>AAAAAAAAAAAAAAAAAAAA</u>
ATP	CCTGGGGGAGTATTGCGGAGGAAGGAAAAAAAAAAAAAAAAAAAA AAAA
c-di-GMP (class I)	TTCTAATACGACTCACTATAGGG TGTCACGCACAGGGCAAACCAT TCGAAAGAGTGGGACGCAAAGCCTCCGGCCTAAACCAGAAGACAT GGTAGGTAGCGGGGTTACCGATGGCAC <u>CCCCAAAAAAAAAAAA</u> <u>AAAAAAAA</u>
c-di-GMP (class II)	TTCTAATACGACTCACTATAGGG TATTTATAGAACTGTGAAGTAT ATCTTAAACCTGGGCACTTAAAGATATATGGAGTTAGTAGTGCAA CCTGCTATAAAT <u>CCCCAAAAAAAAAAAAAAAAAAAA</u>
Glycine	TTCTAATACGACTCACTATAGGG CCTCTGGAGAGAACCGTTTAAAT CGGTGCGCCGAAGGAGCAAGCTCTGCGCATATGCAGAGTGAACTC TCAGGCAAAGGACAGAGGCC <u>CCCCAAAAAAAAAAAA</u> <u>A</u>
TPP (Thi1)	TTCTAATACGACTCACTATAGGG TTGCTAGGAGAGCTGGTGTTC CAGCTGAGAGTAAGACCTTAAAGTCTTTGATCCTTTTTATTACCTGAT CTAGATTATGCTAGCGTAGGGAAGCA <u>CCCCAAAAAAAAAAAA</u>

AAAAAAAA

TPP (*thiM*)

TTCTAATACGACTCACTATAGGGACTCGGGGTGCCCTTCTGCGTG
AAGGCTGAGAAATACCCGTATCACCTGATCTGGATAATGCCAGCGT
AGGGAAGTCCCCAAAAAAAAAAAAAAAAAAAAAAAA

Supporting Information References

- (1) Katsamba, P. S.; Park, S.; Laird-Offringa, I. A. *Methods* **2002**, *26*, 95-104.
- (2) Armbruster, D. A.; Pry, T. *The Clinical biochemist. Reviews / Australian Association of Clinical Biochemists* **2008**, *29 Suppl 1*, S49-52.
- (3) Jenison, R. D.; Gill, S. C.; Pardi, A.; Polisky, B. *Science* **1994**, *263*, 1425-9.
- (4) Burgstaller, P.; Famulok, M. *Angewandte Chemie International Edition in English* **1994**, *33*, 1084-1087.
- (5) Grate, D.; Wilson, C. *Proceedings of the National Academy of Sciences of the United States of America* **1999**, *96*, 6131-6.
- (6) Huizenga, D. E.; Szostak, J. W. *Biochemistry* **1995**, *34*, 656-665.
- (7) Famulok, M. *Journal of the American Chemical Society* **1994**, *116*, 1698-1706.
- (8) Mannironi, C.; Scerch, C.; Fruscoloni, P.; Tocchini-Valentini, G. P. *RNA* **2000**, *6*, 520-7.